sustainability

MDPI

Article

Prediction of Suitable Distribution Area of *Plateau pika* (*Ochotona curzoniae*) in the Qinghai–Tibet Plateau under Shared Socioeconomic Pathways (SSPs)

Yinglian Qi [1], Xiaoyan Pu [2], Yaxiong Li [3], Dingai Li [3], Mingrui Huang [3], Xuan Zheng [3], Jiaxin Guo [3] and Zhi Chen [1,3,*]

[1] School of Geographic Science, Qinghai Normal University, Xining 810008, China
[2] Medical College, Qinghai University, Xining 810016, China
[3] School of Life Science, Qinghai Normal University, Xining 810008, China
* Correspondence: czi58@163.com

Abstract: The Qinghai–Tibet Plateau is one of the regions most strongly affected by climate change. The climate feedback of the distribution of plateau pika, a key species, is closely related to the trophic structure of the plateau ecosystem and the development of agriculture and animal husbandry on the plateau. In order to understand the impact of future climate change on the suitable distribution area of plateau pika, potential suitable distribution areas of *Plateau pika* were predicted using the MaxEnt model under three climate scenarios (SSP 1-2.6, SSP 2-4.5, and SSP 5-8.5) in the near term (2021–2040) and medium term (2041–2060). The predictions were found to be highly accurate with AUC values of 0.997 and 0.996 for the training and test sets. The main results are as follows: (1) The precipitation of the wettest month (BIO 16), mean diurnal range (BIO 2), slope, elevation, temperature seasonality (BIO 4), and annual mean temperature (BIO 1) were the main influencing factors. (2) In the historical period, the total suitable distribution area of *Plateau pika* in the Qinghai–Tibet Plateau accounted for 29.90% of the total area at approximately 74.74 $\times$ 10^4 km^2, concentrated in the eastern and central areas of the Qinghai–Tibet Plateau. (3) The total suitable distribution area of pika exhibited an expansion trend under SSP 1-2.6 and SSP 2-4.5 in the near term (2021–2040), and the expansion area was concentrated in the eastern and central parts of the Qinghai–Tibet Plateau. The expansion area was the largest in Qinghai Province, followed by Sichuan Province and Tibet. In contrast, the suitable distribution area shrank in the Altun Mountains, Xinjiang. Under SSP 5-8.5 in the near term and all scenarios in the medium term (2041–2060), the suitable distribution area of *Plateau pika* decreased to different degrees. The shrinkage area was concentrated at the margin of the Qaidam Basin, central Tibet, and the Qilian Mountains in the east of Qinghai Province. (4) *Plateau pika* migrated toward the east or southeast on the Qinghai–Tibet Plateau under the three climate scenarios. Under most of the scenarios, the migration distance was longer in the medium term than in the near term.

Keywords: Qinghai–Tibet Plateau; MaxEnt; pika; climate change; potential suitable area

Citation: Qi, Y.; Pu, X.; Li, Y.; Li, D.; Huang, M.; Zheng, X.; Guo, J.; Chen, Z. Prediction of Suitable Distribution Area of *Plateau pika* (*Ochotona curzoniae*) in the Qinghai–Tibet Plateau under Shared Socioeconomic Pathways (SSPs). *Sustainability* **2022**, *14*, 12114. https://doi.org/10.3390/su141912114

Academic Editor: Pablo Peri

Received: 2 September 2022
Accepted: 22 September 2022
Published: 25 September 2022

1. Introduction

In August 2021, the United Nations Intergovernmental Panel on Climate Change (IPCC) released the sixth Assessment Report of the Working Group I report "Climate Change 2021: The Physical Science Basis". According to the report, the global surface temperature was 1.09 °C higher in 2011–2020 than that in 1850–1900. Globally averaged precipitation over land has likely increased since 1950, with a higher rate of increase since the 1980s. The rate of melting glaciers is also accelerating. The scale of recent changes across the overall climate system and the present state of many aspects of the climate system are unprecedented with respect to many centuries and many millennia [1]. Against this backdrop of dramatic global climate change, the Qinghai–Tibet Plateau, known as the "roof of the world", the "Third pole of the earth", and the "Water tower of Asia", has

also attracted much attention. According to research [2], the Qinghai–Tibet Plateau has seen the fastest warming in China over the past 60 years. From 1961 to 2020, its annual mean temperature increased by 0.35 °C every decade, with precipitation contributing more than 70%. In addition, more than 80% of the lakes on the plateau have expanded. In the past 50 years, glaciers on the plateau have retreated at an accelerated rate, and its reserves have decreased by 15%, with its area shrinking from 53,000 km^2 to 45,000 km^2. Glaciers in the Himalayas, Hengduan, Nyainqêntanglhaa, and Qilian mountains have shrunk by 20–30%. Dramatic changes in the environment lead to changes in biomes. For example, the influx of lowland species in periglacial areas compresses the living space of indigenous species, changes the relationships among indigenous species, and even changes the network structure of the ecosystem, leading to changes in the structure and function of the ecosystem. Research shows that driven by climate factors, some species, such as macaques [3], *Pomatosace ficula* [4], *Fritillaria Cirrhosae bulbus* [5], *Cordyceps sinensis* [6], and *Sinadoxa corydalifolia* [7], tend to decline in number, whereas other species such as plateau zokor tend to increase [8]. In Qinghai Province; one third of the habitats of wild species are declining, and two thirds are increasing [9]. However, the response of plateau pika, which plays a key role in the ecosystem of the Qinghai–Tibet Plateau [10,11], to future climate change has rarely been reported.

Plateau pika (*Ochotona curzoniae*), also known as the black-lipped pika, is a small non-hibernating phytophagous mammal [10]. In China, it is widely distributed in Qinghai, Tibet, Gansu, and northwest Sichuan and is a keystone species in the Qinghai–Tibet Plateau [11]. It plays an important role in maintaining the stability of the Qinghai–Tibet Plateau ecosystem [10,11]. Pika burrowing can not only provide nests for many small birds and lizards [10] but also increase soil total nitrogen, total phosphorus, and microbial biomass [12], providing more nutrient sources for plant growth and increasing above-ground biomass [13]. At the same time, *Plateau pika* is also the main food source for most small and medium-sized carnivores and almost all raptors on the grassland [14–17]. However, as a burrowing and rapidly breeding rodent, if its population density reaches excessive levels, pika could disrupt grass growth [18] on the plateau and threaten the development of grassland animal husbandry and the survival of other small herbivores. Therefore, studying the potential effects of climate change on *Plateau pika* can help to predict population changes, thereby providing some reference for effectively planning future management strategies and preventing the further degradation of alpine grassland ecosystems.

For researching the potential distribution of species, species distribution models (SDMs) are widely used at present. Those models are numerical tools that predict species distribution by combining the location of species occurrence and the corresponding values of varied environmental variables extracted from spatial databases [19]. A variety of SDMs are available to predict potentially suitable habitats for a species, such as maximum entropy (MaxEnt) [20], genetic algorithm for rule set production (GARP) [21], maximum likelihood method (Maxlike) [22], generalized additive model (GAM) [23], categorical generalized linear model (GLM) [24], and BIOMOD [25]. Studies have shown that the MaxEnt model has better performance than other models, with the ability to better handle the complex interaction between predictor variables and respond to habitat interaction factors in a relatively stable manner [26]. Therefore, it has been widely used in the prediction of potential distribution areas of species and the response of the spatial distribution of species to climate change, as well as the planning of species reserves. According to species distribution points and the corresponding environment variables, and the surrounding environment with maximum entropy in the system of state parameters, the MaxEnt model determines the stability of the relationship between species and the environment to estimate the potential distribution of species and produce a continuous grating prediction map. The produced map represents the habitat suitability of species in the study area with probability values between 0 and 1; the higher the probability is (closer to 1), the more suitable the habitat is [26]. In recent years, the MaxEnt model has achieved good results in the study of the geographical distribution and climate response of many animals and plants, including

blue-eared pheasant (*Crossoptilon auritum*) [27], blood pheasant (*Ithaginis cruentus*) [27], *Artemisia ordosica* [28], Asiatic black bear (*Ursus thibetnaus*) [29], *Rana Hanluica* [30], and European roe deer (*Capreolus Capreolus*) [31]. These studies proved the high applicability of MaxEnt for predicting the distribution of animals and plants.

In this study, the suitable distribution area of *Plateau pika* in the Qinghai–Tibet Plateau was predicted using the MaxEnt model, considering three scenarios (SSP 1-2.6, SSP 2-4.5, and SSP 5-8.5) in the near term (2021–2040) and medium term (2041–2060). The objectives were to: 1. analyze the distribution characteristics of suitable areas of *Plateau pika* under three scenarios in different periods; 2. evaluate the temporal and spatial changes in the potential suitable distribution area of *Plateau pika* under three climate scenarios; 3. clarify the migration direction and distance of *Plateau pika* in the Qinghai–Tibet Plateau under the influence of climate change.

2. Materials and Methods

2.1. Study Area

The Qinghai–Tibet Plateau (73° 20′~104° 20′ E, 26° 10′~39° 0′ N) as shown in Figure 1, is located in the southwest of China, with an area of 2.5 × 10^6 km^2. The terrain is complex, with the average altitude exceeding 4000 m [32]. The annual average temperature in most areas is lower than 0 °C; air oxygen content is low; ultraviolet light is strong; and precipitation is scarce. The coverage, height, biomass, and richness of vegetation are relatively low, forming ecosystems with relatively low stability, such as alpine meadow and alpine grassland [33]. Under the unique climatic characteristics and complex geographical environment, the plateau has developed a unique biodiversity. Studies show that the Qinghai–Tibet Plateau has 14,634 species of vascular plants and 1763 species of vertebrates, representing a region with a concentrated distribution of rare and endangered mammals in China [34–36]. Moreover, it serves as an important ecological security barrier area in China and even Asia. In recent years, with climate change, the suitable distribution areas of many endemic species in the Qinghai–Tibet Plateau are decreasing, owing to which the Qinghai–Tibet Plateau has become a hot spot for studying the conservation of global biodiversity [34,36].

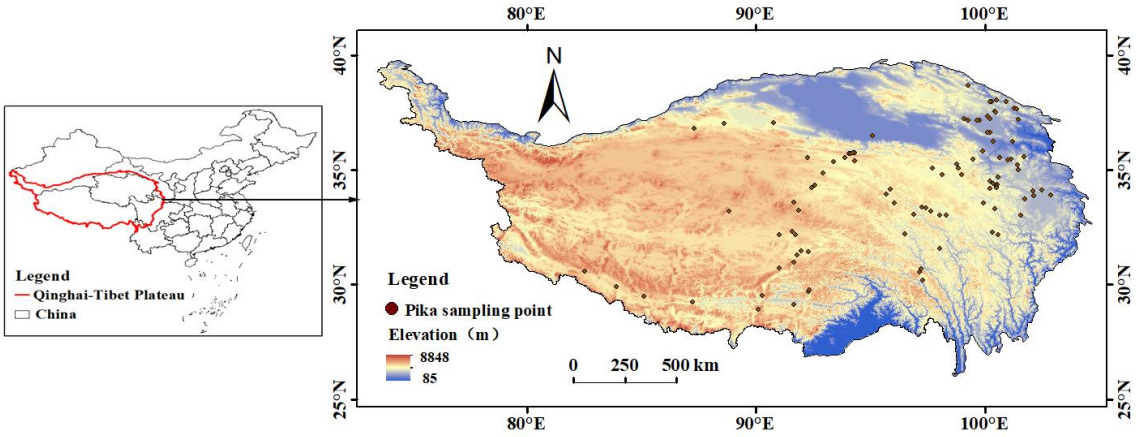

Figure 1. The location of the study area.

2.2. Theoretical Basis and Research Framework

The MaxEnt model adopts the receiver operating characteristic (ROC) curve to test the accuracy of the reconstructed model [20]. The ROC curve determines model accuracy based on non-threshold dependence and changes the judgment threshold. The ROC curve is plotted with the false positive rate (the probability of positive prediction without the actual distribution of the species) as the abscissa and the true positive rate (the probability of positive prediction with the actual distribution of the species) as the ordinate. The area enclosed by the curve and the abscissa is known as the area under the curve (AUC), and its

values lie between 0 and 1. It is used to measure the accuracy of the prediction results of the model, with the following standards: 0.50–0.60, failure; 0.61–0.70, poor; 0.71–0.80, fair; 0.81–0.90, good; 0.91–1.00, excellent [37].

This study was conducted in four main steps: (1). data collection and selection; (2). model optimization; (3). model calculation; (4). result analysis. The specific research framework is shown in Figure 2.

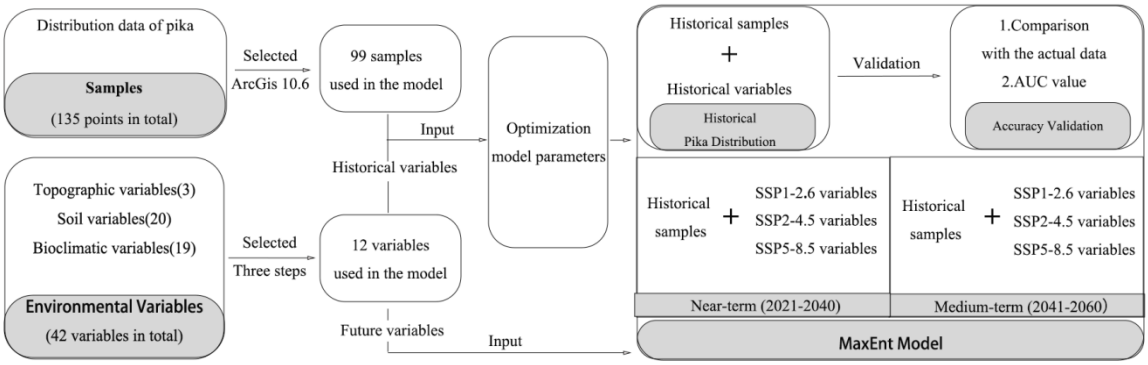

Figure 2. Research framework for the study.

2.3. Data Collection

The MaxEnt model requires input data of species distribution and environmental variables. In this study, the species distribution data were collected from three sources, field surveying of this study in 2020–2021, literature review [38], and the Global Biodiversity Information Facility (https://www.gbif.org/search?q=plateau%20pika, accessed on 27 March 2022). A total of 135 sampling sites were selected. The data were processed to eliminate duplicate, inaccurate, and controversial points. To avoid data over-fitting, the preliminarily screened sampling points were imported into ArcGIS, and the distribution data with a distance of less than 10 km between two points were randomly eliminated [39,40]. Finally, 99 sampling points were selected for model calculation, and the geographic coordinates of the sampling points are detailed in Appendix A, Table A1.

Most scholars only consider the topographic and climatic factors for studying the suitable distribution areas of animals [41–44], but a few scholars believe that the physical and chemical properties of soil are also an environmental variable that cannot be ignored when studying soil-burrowing animals [45]. Therefore, three environmental variables (terrain, climate, and soil) were selected to predict the impact of future climate on the suitable distribution area of *Plateau pika* (Table 1). The results of this study were analyzed under the following three assumptions for the next 40 years: (1). The influence of human activities and other biological factors on *Plateau pika* can be ignored. (2). Changes in soil and topography can be ignored. (3). The traits of *Plateau pika* remain unchanged.

Table 1. Data and sources.

Data Name	Time Resolution	Spatial Resolution	Data Source
Global Digital Elevation Model Data	2010	30 m × 30 m	United States Geological Survey https://topotools.cr.usgs.gov (accessed on 1 October 2019)
Geographic Information System Data of the Scope and Boundary of the Qinghai–Tibet Plateau	2014	-	Global Change Scientific Research Data Publishing System http://www.geodoi.ac.cn (accessed on 1 April 2020)
Global Soil Data	2015	30 s × 30 s	International Soil Reference and Information Centre https://data.isric.org (accessed on 6 April 2022)
Climate Model Data	1971–2099	30 s × 30 s	WorldClim https://www.worldclim.org (accessed on 4 April 2022)

Meteorological data were acquired from a world climate data network (https://www.worldclim.org, accessed on 4 April 2022). Data covering the period from 1970 to 2000 were set as historical data, and future climate data were based on the Sixth International Coupled Model Comparison Program (CMIP 6) implemented by the World Climate Research Program (WCRP), with a spatial resolution of 1 km [46]. The Shared Socioeconomic Pathways (SSPs) proposed by the CMIP 6 provide diverse emission scenarios by considering the stable CO_2 concentration and corresponding radiation intensity in the next 100 years and by combining socioeconomic development pathways, which can provide more reasonable simulation results for mitigation and adaptation research, and regional climate prediction. Therefore, the CMIP 6 model has shown significantly higher climate sensitivity than the CMIP 5 model thus far [47]. In addition, RCP 2.6, RCP 4.5, RCP 6.0, and RCP 8.5 in the CMIP 5 climate model are upgraded to SSP 1-2.6, SSP 2-4.5, SSP 4-6.0, and SSP 5-8.5 in CMIP 6, while new emission models, SSP 1-1.9, SSP 4-3.4, SSP 5-3.4, and SSP 3-7.0, have been added [47–51], thus compensating for the lack of RCP scenarios in CMIP 5 to a large extent. In this study, three scenarios (SSP 1-2.6, SSP 2-4.5, and SSP 5-8.5) were selected to predict the suitable distribution areas in the near term (2021–2040) and medium term (2041–2060).

Soil data were obtained from the ISRIC-WISE 30 SEC data of the International Soil Reference and Information Centre (https://www.isric.org, accessed on 6 April 2022), published in 2015, which complements the ISRIC-Wise Soil Profile database (Batjes 2009, 2011). Approximately 8000 new profiles have been added, resulting in a total of approximately 21,000 profiles. Global regional and national soil information updates (European Soil Database, Soil Map of China, and SOTER- and WISE-derived databases) were combined to produce 30 × 30 arc-second raster maps at a scale of 1:1–1:500,000. In this dataset, the topsoil (0–0.3 m) and subsoil (0.3–1 m) layers in the ISRIC-WISE data are further classified into seven layers: HW30s-WD1–HW30s-WD7, corresponding to depths of 0–0.2, 0.2–04, 0.4–0.6, 0.6–0.8, 0.8–1, 1–1.5, and 1.5–2 m [52]. Some studies have shown that the average cave depth of *Plateau pika* is between 30 cm and 40 cm [53]. Accordingly, the data of HW30S-WD2 (0.2–0.4 m) were extracted using ArcGIS to predict the distribution area of plateau pika.

Many studies have shown that the results of a single climate model are not accurate [54–56]. For the regional mean temperature and precipitation over the whole of China, most climate models underestimate the actual temperature and overestimate precipitation [54]. Therefore, to reduce the errors and uncertainties between different climate model data and make the results more reliable, we averaged the data from eight models using the numpy module and the osgeo module of Python 3.8. The climate models we used to average were ACCESS-ESM 1-5, CanESM 5, FIO-ESM-2-0, EC-Earth 3-Veg, BCC-CSM 2-MR, CMCC-ESM 2, CNRM-CM 6-1, and MRI-ESM 2-0.

2.4. Screening of Environment Variables

To ensure a strong correlation among the various environmental variables used for model prediction and the survival of plateau pikas, 43 (as show in Appendix A, Table A2) candidate variables were screened with the following three steps.

In the first step, the probability distribution of each variable (denoted as X) in the whole Tibetan Plateau and *Plateau pika* distribution area, denoted as P and Q, respectively, was estimated, and the Kullback–Leibler divergence (KL divergence) of P from Q was calculated (Equation (1)). This difference is a measure of the difference between one probability distribution and another [57,58]. If the two distribution probabilities of a variable are highly similar, the variable is considered to have little significance for the distribution of plateau pika. Therefore, all variables with KL divergence less than 1 were eliminated, and the remaining variables were subjected to the next step. The KL divergence can be calculated using the following formula:

$$D(P//Q) = \sum P(X) \log \frac{P(X)}{Q(X)} \quad (1)$$

We extracted the values of the sample points and the whole Qinghai–Tibet Plateau using ArcGIS 10.6 and then calculated the KL divergence of the two groups vlaues with the numpy module in Python 3.8. As shown in Table 2, 18 indicators with KL divergence greater than 1 were obtained.

Table 2. Variables for which the calculation result of KL divergence was greater than 1.

Variable	KL Divergence
Precipitation of wettest quarter (BIO 16)	5.67
Temperature seasonality (standard deviation × 100) (BIO 4)	5.02
Annual precipitation (BIO 12)	4.35
Cation exchange capacity (CECsoil) (CECS)	3.89
Elevation	3.30
Slope	2.56
Annual mean temperature (BIO 1)	2.34
Mean diurnal range (Mean of monthly (max temp–min temp)) (BIO 2)	2.01
Precipitation of driest quarter (BIO 17)	1.56
Exchangeable sodium percentage (ESP)	1.32
Soil reaction (pHH_2O) (PHAQ)	1.31
Mean temperature of warmest quarter (BIO 10)	1.29
Precipitation of coldest quarter (BIO 19)	1.27
Bulk density (BULK)	1.23
Aspect	1.18
Base saturation (as % of CECsoil) (BSAT)	1.12
Total nitrogen (TOTN)	1.06
Total exchangeable bases (TEB)	1.02

In the second step, the 18 factors screened in the first step were input to the MaxEnt model to obtain the contribution rate of each variable, and the data with contribution rates less than 0% were excluded. After the second step screening, 16 factors were found to have contributions greater than 0%, as shown in Table 3.

Table 3. Variables whose contribution rate was greater than 0% after MaxEnt model simulation.

Variable	Contribution	Variable	Contribution	Variable	Contribution	Variable	Contribution
BIO 16	26.2	BULK	10.5	BIO 4	2.3	BIO 1	0.7
BIO 2	15.2	CECS	5.7	TEB	1.5	ESP	0.7
Slope	15	BIO 17	4.8	BIO 12	1.2	BIO 10	0.6
Elevation	11.9	Aspect	2.3	TOTN	0.8	BIO 19	0.4

In the third step, the correlations among the 16 variables selected in the second step were determined, and the calculated results are shown in Figure 3. Among the 16 variables, the correlation coefficients were 0.904 between BIO 1 and BIO 10, 0.973 between BIO 12 and BIO 16, 0.993 between BIO 17 and BIO 19, and 0.939 between TOTN and CECS. The correlation coefficients among other environmental variables were all below 0.8. From the set of environmental variables with correlation coefficients greater than 0.8, the variable with the largest contribution rate to the MaxEnt model was selected as the final prediction variable.

After this three-step screening process, 12 variables were finally retained (Table 4) and input to the MaxEnt model to predict the suitable distribution area of *Plateau pika* on the Qinghai–Tibet Plateau.

2.5. Model Optimization

Regarding the MaxEnt model, most researchers use default parameters to build the model. These default parameters were used by early developers to simulate the current range of 266 species, including birds and reptiles. However, recent studies have found that when the model is operated with default parameters, it is sensitive to sampling bias and prone to overfitting, which affects the transfer ability of the model and results in poor

performance when the model is used to predict potential distribution areas in the context of climate change [59–61]. In order to ensure more accurate predictions, R 3.6.3 combining the Kuenm [62] package (https://github.com/marlonecobos/kuenm/tree/master/replicate_examples accessed on 28 May 2022) was applied to optimize the two main parameters of the MaxEnt model (control frequency doubling (RM) and characteristics combination (FC)) [63]. The complexity of the model under various parameter conditions was analyzed, and the model parameter with the lowest complexity was selected as the optimal model. In this manner, the potential distribution of the species was reasonably predicted. The specific steps are reported below.

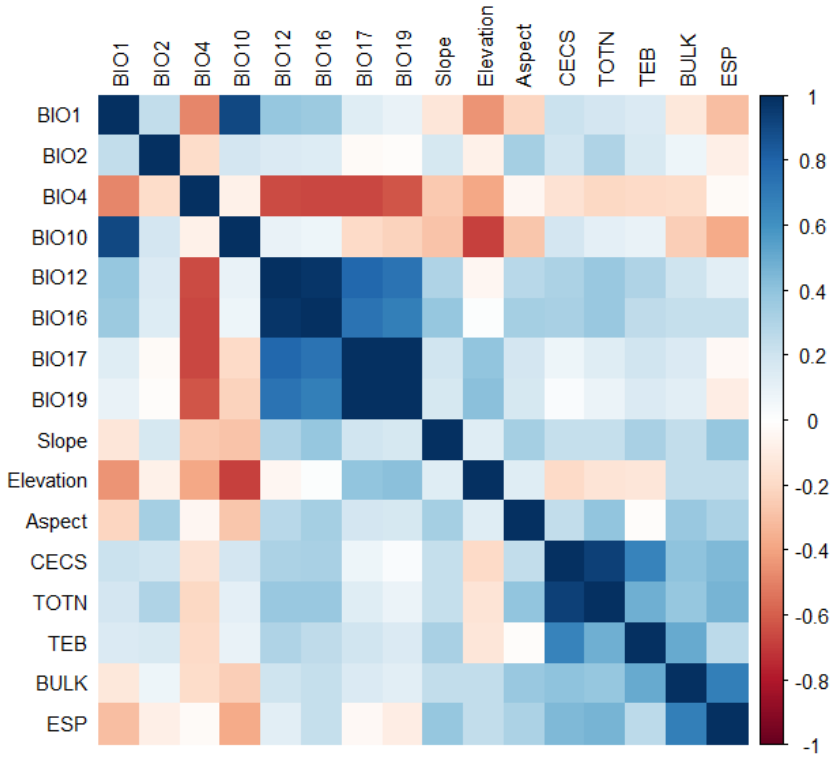

Figure 3. The correlation analysis of modeling variables.

Table 4. The final variables used in the model operation and their contribution rates.

Variable	Contribution	Variable	Contribution	Variable	Contribution	Variable	Contribution
BIO 16	29.8	Elevation	15.5	BIO 17	3.1	BULK	0.4
BIO 2	19.7	BIO 4	8	CECS	2.1	ESP	0.3
Slope	17	BIO 1	3.5	Aspect	0.6	TEB	0.2

First, the regularization multiplier (RM) was set to 0.1–4.0, with a total of 40 RM values increasing by intervals of 0.1. Then, the following 5 features (FCs) were randomly combined into 31 groups: liner-L, Quadratic-Q, Hinge-H, Product-P, and Threshold-T. Finally, 1160 candidate models were generated by combining the 40 RM values and 31 characteristic types of FCs to test the fitting effect of *Plateau pika* distribution data. The evaluation of the candidate model using this package is primarily based on the significance level of the calculation results, omission rate, and model complexity. The model with statistically significant values, low omission rate, and minimum complexity was selected as the optimal model. In the Kuenm package, the mean AUC ratio (Mean-AUC ratio) and pval_pROC were used to measure the level of statistical significance. Mean-AUC ratio > 1 and pval_pROC close to the minimum value of 0 indicate statistical significance [59]. Omission_rate_at_5% represents the omission rate. The lower the Omission_Rate_AT_5% is, the more accurate the model results are. The Akaike Information Criterion (delta AICc) can reflect the model

fit and complexity [60]. It is a standard for measuring the goodness of model fit. Generally, the delta AICc value is close to 0, and the lower the complexity of the model is, the better the model fit is [64,65]. According to the results, two candidate models met the selection conditions (Table 5). According to this principle [65], the RM value of 1.1 and the feature-type combination of QT were selected as the best model parameters for subsequent calculations.

Table 5. Statistical results of model optimization.

FC	RM	Mean_AUC_Ratio	Pval_pROC	Omission_Rate_at_5%	Delta_AICc
QT *	1.1	1.609203	0	0	0
QT *	1.2	1.599023	0	0	1.922811
Default	1	1.514370355	0	0.125	296.294

* The good parameter combination selected using the Kuenm package. Default stands for the MaxEnt default parameter combination.

3. Results

3.1. Model Accuracy Test and Identification of Main Environmental Factors

In this study, 99 sampling points and 12 environmental variables were imported into the MaxEnt model. In general, 75% of the sampling points were randomly selected as the training set and 25% as the test set, and the feature class was set as the QT combination. The regularization multiplier was 1.1, with 10 repetitions, and other parameters were set as the default. According to the results, the AUC of the training set and test set of *Plateau pika* were 0.997 and 0.996, respectively as shown in Appendix B, Figure A1, indicating the good prediction performance and high reliability of the MaxEnt model.

The final calculation results of the 12 environmental variables (as shown in Table 4) showed that the main factors affecting the distribution of *Plateau pika* in the Qinghai–Tibet Plateau were meteorological factors and topographic factors, accounting for 64.1% and 33.1%, respectively, while soil factors contributed less, accounting for 3%. Among the factors, BIO16, BIO2, Slope, Elevation, BIO 4, and BIO 1 were the main influencing factors. A single-factor response curve was used to investigate the relationship between the potential distribution probability of *Plateau pika* and the main environmental factors. When the potential distribution probability of *Plateau pika* was >0.5, the wettest quarterly precipitation (BIO 16) was 90.13–420.58 mm. The mean annual temperature (BIO 1) was −4.65–2.88 °C; the mean daily temperature range (BIO 2) was 13.31–15.69 °C, seasonal variation coefficient of air temperature (BIO 4) was 663.94–911.72 (×100), elevation was 3037.09–4790.37 m, and slope was >15.20°. The quantitative analysis of each factor threshold showed that suitable habitats of *Plateau pika* are located in areas with high altitude, low temperature, and certain slope (Appendix B, Figure A2).

3.2. Suitable Distribution Area of Plateau pika under Historical Climatic Conditions

The potential suitable distribution areas of *Plateau pika* during the historical period (1970–2000), the near term (2021–2040), and the medium term (2041–2060) were estimated using the MaxEnt model. The MaxEnt model outputs raster data in ASCII format. The grid cell value represents the distribution probability (p), which ranges from 0 to 1. In order to describe spatial differences in the distribution of plateau pika, the distribution probability was set to range from 0% to 100%. According to the criteria of possibility classification in the IPCC evaluation report and existing research results [6,66], the distribution range was divided into four grades: unsuitable area ($p < 22\%$), minimally suitable area ($22\% \leq p < 50\%$), moderately suitable area ($50\% \leq p < 75\%$), and highly suitable area ($75\% \leq p < 1$).

The results showed that the total suitable distribution area of *Plateau pika* in the Qinghai–Tibet Plateau was approximately 74.74×10^4 km^2, accounting for 29.90% of the total area (Table 6) and concentrated in the eastern and central areas of the Qinghai–Tibet Plateau (Figure 4). The highly suitable area, moderately suitable area, and minimally suit-

able area covered approximately 13.62 × 10^4 km^2, 36.32 × 10^4 km^2, and 134.28 × 10^4 km^2, accounting for 5.45%, 8.20%, and 16.24%, respectively.

Table 6. The suitable distribution area of *Plateau pika* in different grades according to different climate models.

Time		TSA	U-SA	Mi-SA	Mo-SA	H-SA
Historical Period		29.90%	70.10%	16.24%	8.20%	5.45%
Near term	SSP 1-2.6	31.02%	68.98%	16.5%	8.73%	5.79%
	SSP 2-4.5	32.97%	67.03%	16.88%	9.43%	6.67%
	SSP 5-8.5	26.09%	73.91%	14.15%	6.97%	4.96%
Medium term	SSP 1-2.6	28.78%	71.22%	15.01%	7.99%	5.78%
	SSP 2-4.5	28.87%	71.13%	15.26%	7.81%	5.8%
	SSP 5-8.5	28.15%	71.85%	15.98%	7.2%	4.97%

T-SA stands for total suitable area; U-SA stands for unsuitable area; Mi-SA stands for minimally suitable area; MO-SA stands for moderately suitable area; H-SA stands for highly suitable area.

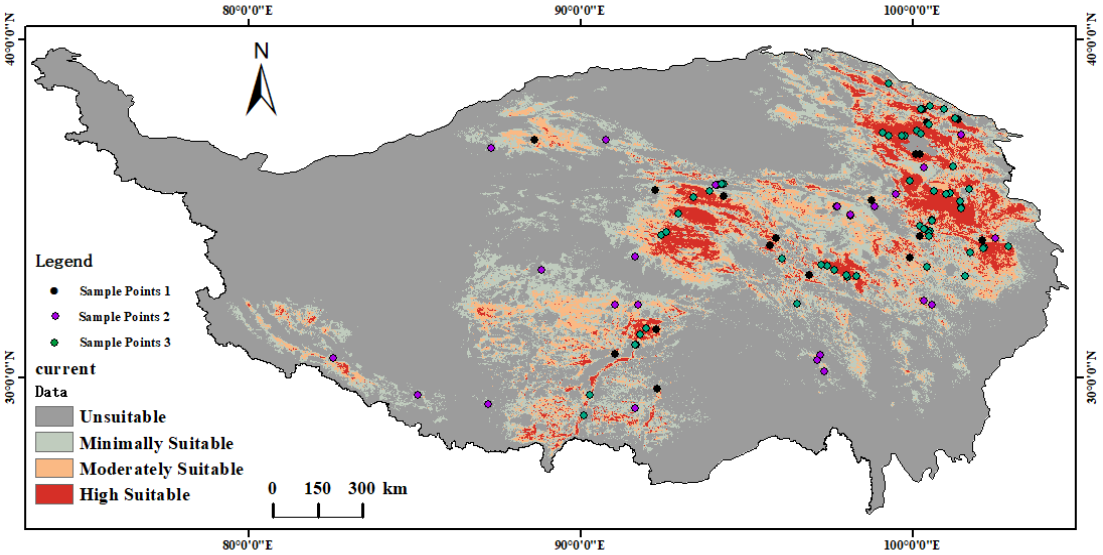

Figure 4. Distribution of potential suitable areas for *Plateau pika* on the Qinghai–Tibet Plateau in the historical period.

The accuracy of the estimation results of the potential distribution area of pika on the Qinghai–Tibet Plateau was verified as follows:

- The 99 sampling points were projected onto the raster map of the historical prediction results, and the fitness index of each sampling point was extracted. The results showed that 61.61%, 25.25%, and 15.15% of the points were distributed in the highly suitable, moderately suitable, and minimally suitable areas, respectively, whereas no points were distributed in the unsuitable area. The proportion of distribution points of *Plateau pika* decreased with the decrease in suitability;
- The effective burrow density of *Plateau pika* in 76 sample plots was counted during sampling. The effective burrow density can represent the population density of *Plateau pika* [67]. The statistical results showed that the average effective burrow density was 0.276 ± 0.013 m^{-2} for the sampling points in the highly suitable area (Figure 4, Sample 3), approximately 0.152 ± 0.015 m^{-2} for the sampling points in the moderately suitable area (Figure 4, Sample 2), and 0.078 ± 0.005 m^{-2} for the sampling points in the minimally suitable area (Figure 4, Sample 1). The effective burrow density decreased with the decrease in suitability.

These results indicate that the model predictions agree with the actual distribution of plateau pika. This means that the estimated results for potential suitable areas of *Plateau pika* in the historical period on the Qinghai–Tibet Plateau are reasonably accurate.

3.3. Suitable Distribution Area of Plateau Pika on the Qinghai–Tibet Plateau under Three Climate Change Scenarios

Under the SSP 1-2.6, SSP 2-4.5, and SSP 5-8.5 scenarios, the potential distribution areas of *Plateau pika* in the near term and medium term were mainly concentrated in the eastern and central regions of the Qinghai–Tibet Plateau (Figure 5), and most of the highly suitable areas were in Qinghai Province (Appendix B, Figure A3), with a small distribution in the northern side of the Himalayas. The minimally suitable areas were mainly distributed in western Sichuan Province, Tibet, and southern Gansu Province.

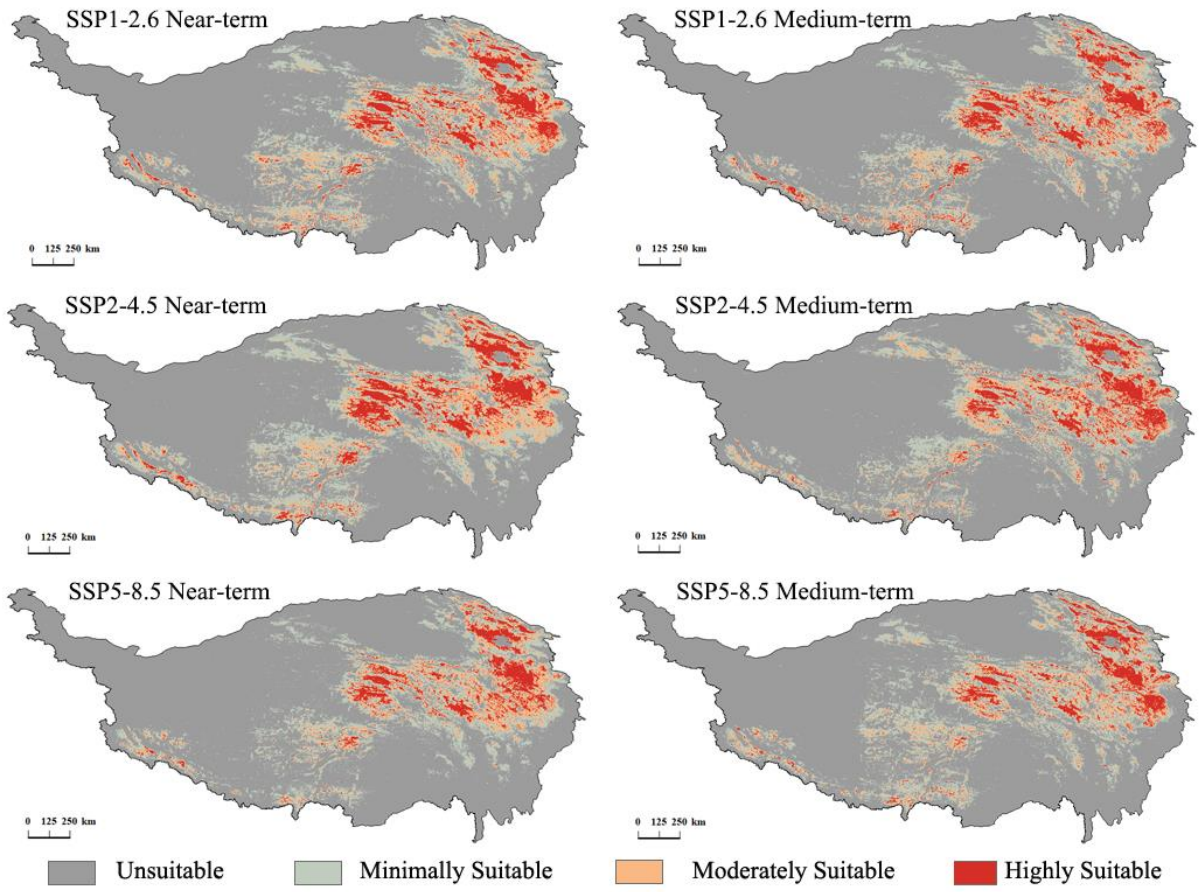

Figure 5. Distribution of potential suitable areas for *Plateau pika* on the Qinghai–Tibet Plateau in the near term and medium term.

As shown in Table 6, under the three climate scenarios in the near and medium terms, prominent differences were observed among areas with different grades of suitability. In the near term, the total suitable area under SSP 1-2.6 and SSP 2-4.5 increased by 1.12% (approximately 3.00×10^4 km^2) and 3.02% (approximately 7.50×10^4 km^2), respectively, compared with the historical period. Under SSP 1-2.6, highly, moderately, and minimally suitable areas increased by 0.34% (0.85×10^4 km^2), 0.53% (1.33×10^4 km^2), and 0.26% (0.65×10^4 km^2) with respect to the total area, respectively. Under SSP 2-4.5, highly, moderately, and minimally suitable areas increased by 1.22% (approximately 4.6×10^4 km^2), 1.22% (approximately 2.48×10^4 km^2), and 0.64% (approximately 1.6×10^4 km^2), respectively. Under SSP5-8.5, the total suitable area showed a shrinking trend, decreasing by 3.81% (approximately 9.53×10^4 km^2), compared with the historical period. Specifically, highly, moderately, and minimally suitable areas shrank by 0.49% (approximately 1.22×10^4 km^2), 1.23% (approximately 3.08×10^4 km^2), and 2.09% (approximately 7.25×10^4 km^2), respectively.

In the medium term, the total suitable distribution area showed a decreasing trend under SSP 1-2.6, SSP 2-4.5, and SSP 5-8.5, with decreases accounting for 1.12% (approxi-

mately 2.80 × 10^4 km^2), 1.03% (approximately 2.57 × 10^4 km^2), and 1.75% (approximately 4.38 × 10^4 km^2) of the total area, respectively. Under SSP 1-2.6 and SSP 5-8.5, the distribution of areas with different suitability grades also showed different degrees of reduction. Under SSP 2-4.5 and SSP 1-2.6, the areas of moderately and minimally suitable areas showed a decreasing trend, but the areas of highly suitable areas showed a slight increasing trend, accounting for 0.33% (approximately 0.83 × 10^4 km^2) and 0.35% (approximately 0.88 × 10^4 km^2) of the total area, respectively. This indicated that a small portion of moderately and minimally suitable areas transformed into highly suitable areas under these climate scenarios.

Overall, the suitable distribution area of *Plateau pika* in the Qinghai–Tibet Plateau expanded under SSP 1-2.6 and SSP 2-4.5 in the near term, and but it shrank to different degrees in other periods and scenarios. Among them, the largest shrinkage occurred under SSP 5-8.5.

3.4. Geospatial Analysis of Suitable Distribution Area of Plateau Pika

To intuitively understand changes in the suitable area of plateau pika, areas having a suitability index greater than 0.5 were compared with the historical suitable area. The results showed that the spatial changes in the suitable area generally remained similar in the near term and medium term (Figure 6), without any significant changes in most areas. Nevertheless, a small portion of suitable distribution areas expanded or shrank to varying degrees.

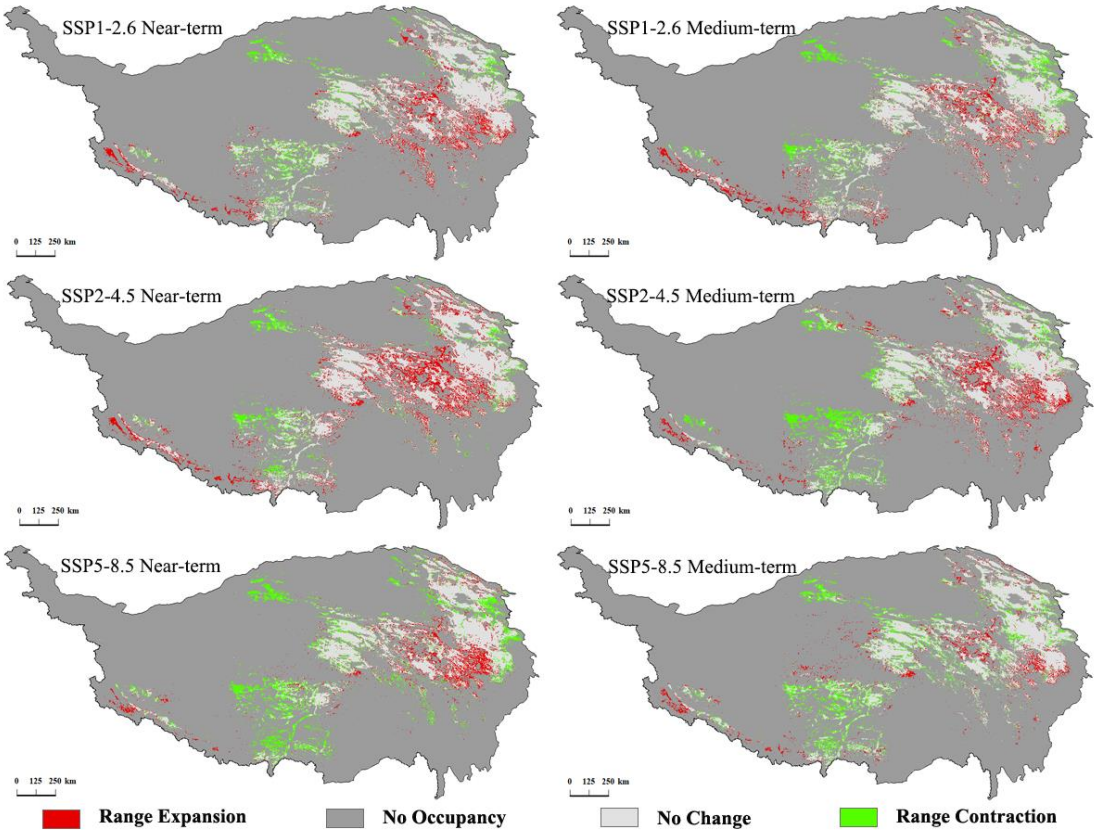

Figure 6. Spatial changes in potential suitable areas of *Plateau pika* on the Qinghai–Tibet Plateau.

In the near term, the expansion of the potential suitable area was the largest under SSP 2-4.5, accounting for 4.42% of the total area of the Qinghai–Tibet Plateau (Figure 6 and Appendix B, Figure A4) and being mainly concentrated in the south of Qinghai Province and the Zoige grassland area in the northwest of Sichuan Province. In addition, the expansion trend was also prominent in the northern part of the Himalayas. Similar to that

under SSP 2-4.5, the second largest expansion occurred under SSP 1-2.6, with the increased area accounting for 3.08% of the total area. The expansion was the smallest under SSP 5-8.5, accounting for only 2.52% of the total area. The expansion area was mainly concentrated in the Animaqing mountain and Bayankala mountain in the southeast of Qinghai Province. The shrinkage of the potential suitable area followed the order SSP 5-8.5 (4.27%) > SSP 1-2.6 (2.15%) > SSP 2-4.5 (1.95%). The shrinkages under SSP 1-2.6 and SSP 2-4.5 were similar and mainly concentrated at the margin of the Qaidam Basin, central Tibet, and the Qilian Mountains in the east of Qinghai Province.

In the medium term, the expansion was the largest under SSP 1-2.6 and SSP 2-4.5, accounting for 2.79% and 3.07% of the total area, respectively (Appendix B, Figure A4). Under SSP 1-2.6, the expansion was mainly concentrated in the southwest of Qinghai Province and the southwest of Tibet (Figure 6). The expansion under the SSP 2-4.5 was mainly concentrated in the southeast of Qinghai Province. The smallest expansion was observed under SSP 5-8.5, accounting for 1.93% of the total area and being mainly concentrated in the southeast of Qinghai Province. The smallest shrinkage was observed under SSP 1-2.6, accounting for 2.60% of the total area. The largest shrinkage was observed under SSP 5-8.5, accounting for 3.43% of the total area. The shrinkage was similar to that in the near term and was mainly concentrated in the southeast of Qinghai Province.

At the provincial level (Appendix B, Figure A4), Qinghai Province showed the largest area of expansion under all scenarios, followed by Tibet and Sichuan Province. The suitable distribution area in Xinjiang showed a shrinking trend, and the expanded and unchanged areas in Xinjiang under the three scenarios were almost 0.

3.5. Centroid Migration Analysis

As shown in Appendix B, Figure A5, the centroids of plateau pikas in the Qinghai–Tibet Plateau migrated eastward or southeastward under different climatic conditions during different periods. Among them, the prediction results under SSP 5-8.5 in the near term and SSP 2-4.5 and SSP 5-8.5 in the medium term were similar. *Plateau pika* migrated eastward, with migration distances of 73.96 km, 124.59 km, and 122.11 km, respectively. The prediction results under SSP 1-2.6 and SSP 2-4.5 in the near term and SSP 1-2.6 in the medium term were similar. *Plateau pika* migrated toward the southeast, with migration distances of 56.17 km, 32.80 km, and 41.80 km, respectively. From the analysis of different time scales, the migration distance under SSP 1-2.6 in the medium term was 17.79 km shorter than that in the near term. In other climate scenarios, the migration distance in the medium term was prolonged to varying degrees; under SSP 2-4.5, it was prolonged by 91.79 km with respect to that in the near term, and under SSP 5-8.5, the extension was 48.14 km. From the analysis of different scenarios, the migration distance was the longest under SSP 2-4.5 in the medium term, at approximately 124.59 km, and it was the shortest under SSP 2-4.5 in the near term, at approximately 32.80 km.

4. Discussion

4.1. Adjustment of Model Accuracy

In order to improve the prediction accuracy of a model, many scholars begin optimization by selecting distribution point data and environmental variables. For example, in order to avoid the low prediction accuracy caused by the over-fitting of species distribution points, Evans [39] and Boria [40] eliminated distribution points at relatively close distances. Based on the analysis of the correlation coefficient between environmental variables and the contribution rate of each variable to the MaxEnt model, Zhang [68] and Wu [69] excluded variables with large correlation coefficients and low contribution rates. On this basis, Su [57] and Ma [58] calculated the KL divergence of the environmental variables and eliminated the variables with KL divergence lower than 1 to optimize the variables. All these measures can improve model accuracy to a certain extent. In addition to the above screening of distribution points and environmental variables, this study also optimized the model parameters. Currently, the commonly used MaxEnt model parameter optimization

tools are the ENMeval [70] and Kuenm packages [62] in R language. Although the two data packages select the best model according to the complexity and fitting degree of various parameter combinations, their respective reference evaluation indexes are slightly different. For example, AUC.diff (equal to AUCtrain-AUCtest) and OR_{10} are used to test the fitting degree of the model to the distribution points of native species. Delta.AICc is used to test the complexity and fitting degree of the model [70]. The Kuenm package adopts Omission_rate_at_5% and AIC to reflect the model fit and complexity, and the Mean-AUC Ratio and pval_pROC to measure the level of statistical significance [62]. Compared with ENMevl, Kuenm includes more evaluation indexes. Therefore, this study used the Kuenm package to adjust the model parameters. After the optimization of the above aspects, the AUC of the final training set and test set were found to be 0.997 and 0.996, respectively, indicating the high performance and precision of the MaxEnt model.

4.2. Key Factors Affecting the Distribution of Plateau Pika

In this study, the variation in the suitable distribution area of *Plateau pika* under different climate conditions was investigated by considering climate, topography, and soil as environmental variables. The contribution rate of each variable to the model followed the order climate variable (64.1%) > topography variable (33.1%) > soil variable (3%). This may be explained by the fact that climate and topography have direct effects on animals, whereas soil indirectly affects the distribution of animals by affecting plants. The contribution of climate variables followed the order precipitation of wettest season (BIO 16) > mean diurnal range (BIO 2) > temperature seasonality (BIO 4) > annual mean temperature (BIO 1) > precipitation in the driest season (BIO 17). This ordering indicates that *Plateau pika* is the most sensitive to precipitation in the driest season. The optimal distribution interval was 90.13–420.58 mm. WU [69] and Calkins [41] showed that precipitation during the driest and wettest seasons significantly contribute to the distribution of pika. On the one hand, appropriate precipitation in the driest and wettest seasons may satisfy the basic water demand of plateau pika. On the other hand, studies showed that appropriate precipitation increases soil water content and reduces soil compaction, which are conducive to the construction of burrows by soil-burrowing animals [69]. The results of several temperature factors, such as BIO 2, BIO 4, and BIO 1, indicated that the low annual mean temperature (−4.65–2.88 °C), the large seasonal coefficient of temperature variation (663.94–911.72), and the large average daily range (13.31–15.69) are favorable for plateau pika. It is possible that plateau pika, similar to American pika, has a high body temperature (40.1 °C) [71], thicker fur, and a relatively weak heat dissipation mechanism. Therefore, it is more suited to living in low-temperature environments with a large average daily range and seasonal variation in the temperature. This is also confirmed by the observation that its activity is deliberately lowered in high-temperature environments [72]. Among the topographic factors, altitude significantly affects the distribution of plateau pika, which is similar to the study by Wu [69]. As shown in Appendix B, Figure A2, the suitable altitude range for the survival of *Plateau pika* is 3037.09–4790.37 m. The oxygen content and the temperature of air vary with altitude. *Plateau pika* has evolved a series of special physiological mechanisms to adapt to the plateau habitat under the long-term low-temperature and low-oxygen environment [73]. This adaptation to such a specific environment may make it unsuitable for survival at low altitudes and high temperatures. Furthermore, the sharp decline in oxygen content and air temperature, and the low content of above-ground biomass at excessively high altitudes may be unsuitable for the survival of a large number of plateau pikas. Another terrain factor is slope. In this study, the optimal growth index of *Plateau pika* was found to be positively correlated with slope. On the one hand, a certain range of slope is conducive to burrowing. On the other hand, steep slopes can broaden the field of vision, which is conducive to being hunted by predators [74]. In addition to soil bulk density (BULK density), which may affect the mining speed of *Plateau pika* and thus its distribution [75], other factors may indirectly affect the distribution of *Plateau pika* by affecting the distribution of plants and other factors. For example, some studies showed

that soil organic carbon content is negatively correlated with cation exchange capacity (CECS) [76]. Wei [77] showed that soil with low organic matter content is more suitable for plateau pikas.

4.3. Change Trend of Suitable Distribution Area of Plateau Pika under Three Climate Scenarios

The three climate scenarios mainly considered future changes in the temperature and precipitation by budgeting the emissions of greenhouse gases such as CO_2. Owing to the different adaptability of wild animals to temperature and precipitation factors, the suitable distribution areas of wild animals on the Qinghai–Tibet Plateau show the trend of expansion, reduction, or migration in response to future climate change. Moreover, the change trend of the suitable distribution areas of the same species also differ under different climate conditions. For example, the suitable distribution area of white-lipped deer (*Cervus albirosrostris*) [78] showed an expansion trend under SSP 1-2.6, whereas it shrank to different degrees under SSP 2-4.5 and SSP 5-8.5. The suitable distribution areas of Marco Polo sheep [41] and wild donkey [79] showed an expansion trend under RCP 2.6 and a reduction trend under RCP 4.5 and RCP 5.8. The Tibetan antelope [79] showed a decreasing trend under the three scenarios. The suitable distribution area of plateau zokor [8] showed an expansion trend under RCP 4.5. The results of this study showed that the total suitable distribution area of *Plateau pika* also showed an expansion trend under SSP 1-2.6 and SSP 2-4.5 in the near term. Under the other scenarios and periods, it showed different degrees of shrinkage. In conclusion, most wild species in the Tibetan Plateau showed an expansion trend under SSP 1-2.6 and RCP 2.6, and the suitable distribution area gradually decreased with the further increase in greenhouse gas emissions. This expansion may be because the temperature and precipitation under SSP 1-2.6 and RCP 2.6 are in the most suitable range for wildlife in the Qinghai–Tibet Plateau. However, with further increases in CO_2 emissions and the passage of time, the temperature rise is predicted to further increase, due to which the population of *Plateau pika* would decrease.

4.4. Comparison of Centroid Transfer in Suitable Distribution Areas of Plateau pika under the Influence of Future Climate Change

Under the influence of climate change, the western and eastern regions of the Qinghai–Tibet Plateau presented completely different environmental characteristics. The western region became dry and warm, leading to the decline in plant productivity [80], while precipitation in the central and eastern regions increased, leading to the advancement of the vegetation greening period and the delaying of the yellow period, thus increasing total productivity [81]. As a result, many wild animals migrated in different directions and at different speeds according to their different selectivity to climate conditions. For example, the migration direction of wild donkeys, Tibetan antelopes, and other ungulates [79,82] was northbound, and that of Marco Polo sheep [42] was westbound under RCP 4.5 and RCP 8.5, but they shifted to the southeast under RCP 2.6. Junhu Su et al. [8] found that Alpine zokors at low altitudes migrated to the southwest under future climate conditions. In addition to wild animals, many plants, such as *Meconopsis punicea* [83] and *Lycium ruthenicum Murr* [68], also showed a trend of southeast migration. In this study, the centroid of the appropriate area of *Plateau pika* in the Qinghai–Tibet Plateau was located in the middle of the Tanggula Mountains and Bayan Har Mountains under the historical climate scenario (Appendix B, Figure A5), but it migrated to the east or southeast under the three future climate scenarios. This is in agreement with the migration direction of some low-altitude plateau zokors reported by Junhu Su [8]. This may be attributable to the gradual increase in the temperature and precipitation, which would promote plant productivity in the southeast of the Qinghai–Tibet Plateau. Meanwhile, the advancement of soil thawing time would favor hunting and burrowing for plateau pika. From the micro perspective, this migration is the response of *Plateau pika* to future climate change, which is conducive to the continuation of *Plateau pika* population. However, from the macro perspective, this migration may pose certain threats to the ecology of the Qinghai–Tibet Plateau. On the

one hand, *Plateau pika* is the main food source for many plateau carnivores and plays a large role in maintaining the plateau food chain as a primary consumer in the plateau ecosystem. Therefore, the migration of *Plateau pika* niche to the southeast would lead to the survival crisis of other highly trophic wild animals in the western region of the plateau, thus reducing biodiversity in the western region of the Qinghai–Tibet Plateau. On the other hand, the core area after eastward migration would be mainly concentrated in the source area of the Yellow River and the junction of the Qinghai Province and Sichuan Province. This would induce grassland destruction and degradation due to the large increase in the population density of *Plateau pika* and affect the development of animal husbandry in this area. Therefore, according to the research results, protection measures should be strengthened for plateau pikas in the western part of the Qinghai Tibet Plateau in the future. At the same time, the prevention and control of rodents should be strengthened in the eastern and southeastern parts of the Qinghai–Tibet Plateau.

5. Conclusions

(1) The election of species distribution points and environmental variables as well as the optimization of MaxEnt model parameters using the Kuenm package could vastly improve the accuracy of model prediction. The environmental factors affecting the distribution of *Plateau pika* in the Qinghai–Tibet Plateau were mainly climatic factors and topographic factors, accounting for 64.1% and 33.1%, while soil factors had a small contribution, accounting for 3%. Specifically, the main influencing factors were BIO 16, BIO 2, Slope, Elevation, BIO 4, and BIO 1.

(2) In the historical period, the total suitable distribution area of *Plateau pika* in the Qinghai–Tibet Plateau accounted for 29.90% (approximately 74.74×10^4 km^2) of the total area (Table 6), concentrated in the eastern and central areas of the Qinghai–Tibet Plateau.

(3) The influence of future climate on the suitable distribution area of *Plateau pika* showed different trends under different scenarios and periods. The total suitable distribution area of pika under SSP 1-2.6 and SSP 2-4.5 showed an expansion trend in the near term (2021–2040), and the expansion area was mainly concentrated in the eastern and central parts of the Qinghai–Tibet Plateau. The expansion was the largest in Qinghai Province, followed by Sichuan Province and Tibet, and the suitable distribution area shrank in the Altun Mountains, Xinjiang. Under SSP 5-8.5 in the near term and all scenarios in the medium term (2041–2060), the suitable distribution area of *Plateau pika* decreased to different degrees. The shrinkage was mainly concentrated at the margin of the Qaidam Basin, central Tibet, and the Qilian Mountains in the east of Qinghai Province.

(4) *Plateau pika* migrated toward the east or southeast on the Qinghai–Tibet Plateau under the three climate scenarios in the future, and under most of the scenarios, the migration distance was longer in the medium term than in the near term.

Author Contributions: Y.Q. conducted the research study, analyzed the data, and wrote the paper; X.P. made suggestions to this paper; Y.L. helped to edit the paper; D.L. processed the data; M.H. helped to process the data; X.Z. helped to edit the paper; J.G. process the data; Z.C. guided the research study and performed extensive updating of the manuscript. All authors have read and agreed to the published version of the manuscript.

Funding: This research study was funded by Qinghai Provincial Key Laboratory of Medicinal Animal and Plant Resources of the Qinghai-Tibetan Plateau (2020-ZJ-Y04).

Institutional Review Board Statement: Not applicable.

Informed Consent Statement: Not applicable.

Data Availability Statement: All data and materials are available upon request.

Acknowledgments: We are particularly indebted to Xufeng Mao from Qinghai Normal University and Jiapeng Qu from Northwest Institute of Plateau Biology for their constructive suggestion on an earlier draft of this paper.

Conflicts of Interest: The authors declare no conflict of interest.

Appendix A

Table A1. Geographical coordinates of sampling points.

Sampling Point	Longitude (°E)	Latitude (°N)	Elevation (m)	Sampling Point	Longitude (°E)	Latitude (°N)	Elevation (m)
Basu1	97.130	30.530	4125	Shiqu2	98.015	33.033	4302
Tibet3	82.536	30.587	4955	Balongnong	98.027	31.565	3942
Naqu5	83.917	29.917	4711	Shiqu3	98.047	32.984	4507
Tibet4	85.089	29.493	4686	Xingxinghai	98.130	34.830	4217
Tibet1	87.218	29.237	4503	Maduo	98.133	34.796	4306
Tuzilake	87.308	36.800	4734	Shiqu4	98.317	33.017	3986
Aqikelake	88.610	37.033	4340	Huashixia1	98.760	35.264	4099
Doublelake	88.832	33.186	4916	Huashixia2	98.850	35.080	4289
Jiangzi	90.101	28.901	4976	Xinghai1	99.000	34.800	4584
Nuni	90.270	29.502	4081	Tianjun	99.106	37.245	3376
kaerqiuka	90.755	37.043	4163	Xinghai2	99.484	35.450	4099
Anduo1	91.035	32.178	4743	Gangcha1	99.667	37.167	3304
Namucuo	91.035	30.721	4844	Niaodao	99.758	37.171	3302
Dangxiong	91.040	30.720	4850	Heka	99.908	35.821	3902
Anduo2	91.590	32.310	4870	Dari1	99.928	33.564	4129
Naqu1	91.650	30.983	4717	Gangcha2	100.134	37.325	3302
Geladandong	91.652	33.589	4856	Jiangxigou	100.211	36.621	3302
Langkazi	91.652	29.109	4334	Maqin1	100.212	34.505	3849
Anduo3	91.718	32.157	4810	Gande	100.218	34.203	4228
Naqu2	91.797	31.280	4608	Mole1	100.233	37.967	3653
Tanggulamountain	91.856	33.224	4860	Qinghailake	100.233	37.233	3302
Naqu3	91.967	31.467	4617	Shiqu2	98.015	33.033	4302
Zhuonailake	92.260	35.548	4680	Mole2	100.299	37.963	3781
Naqu4	92.277	31.441	4471	Seda1	100.325	32.274	3885
Mozhugongka	92.296	29.693	4718	Seda2	100.350	36.233	2973
Riduovillage	92.317	29.767	4785	Dawu	100.350	34.400	3870
Tuotuo River1	92.440	34.216	4536	Reshui	100.434	37.548	3554
Tuotuo River2	92.591	34.330	4591	Dari2	100.437	33.293	3994
Beilu River	92.942	34.862	4572	Qika	100.498	34.207	3977
Chumaer River	93.386	35.356	4517	Maqin2	100.500	34.285	4110
Budong Spring	93.897	35.522	4615	Qilianarou	100.525	38.048	3104
Xidatan1	94.058	35.712	4590	Maqin3	100.533	34.350	4000
Kunlong Mountain1	94.060	35.710	4590	Anduo4	100.590	32.180	4120
Xidatan2	94.135	35.717	4446	Jungong	100.592	34.647	3435
Xidatan3	94.233	35.733	4280	Guinan1	100.633	35.533	3336
Kunlong Mountain2	94.310	35.374	4641	Qilianebao	100.934	37.968	3435
Naqu6	95.083	36.500	2941	Senduo	101.000	35.440	3404
Zhiduo1	95.696	33.939	4367	Guinan2	101.133	35.467	3497
Qumalai	95.877	34.139	4384	Guide1	101.205	36.254	3686
Zhiduo2	96.060	33.540	4350	Menyuan1	101.275	37.690	3263
Nangqian	96.508	32.190	3951	Menyuan2	101.440	35.218	3933
Yushu1	96.886	33.057	3913	Zeku	101.450	35.017	3696
Bangda	97.128	30.529	4355	Lajimountain	101.467	37.200	3661
Basu2	97.206	30.674	4474	Aba	101.581	33.009	3465
Chenduo	97.240	33.360	4432	Tongren	101.716	35.586	3877
Yela Mountain	97.295	30.187	4527	Maqu	101.733	33.717	3521
Basu3	97.330	30.190	4392	Lvqu	102.098	34.065	3716
Yushu2	97.420	33.330	4215	Hequ	102.483	34.133	3612
Shiqu1	97.650	33.183	4361	Ruoergai	102.880	33.900	3490
Elinlake	97.720	35.070	4278				

Table A2. Variables used to estimate the potential suitable area of highland barley.

Data Category	Data Name	Variable Abbreviation	Variable Meaning
Climate data	NASA Earth Exchange Global Daily Downscaled Projections (NEX-GDDP)	BIO 1	Annual mean temperature
		BIO 2	Mean diurnal range (mean of monthly (max temp–min temp))
		BIO 3	Isothermality (BIO 2/BIO 7) (×100)
		BIO 4	Temperature seasonality (standard deviation ×100)
		BIO 5	Max temperature of warmest Month
		BIO 6	Min temperature of coldest Month
		BIO 7	Temperature annual range (BIO 5-BIO 6)
		BIO 8	Mean temperature of wettest quarter
		BIO 9	Mean temperature of driest quarter
		BIO 10	Mean temperature of warmest quarter
		BIO 11	Mean temperature of coldest quarter
		BIO 12	Annual precipitation
		BIO 13	Precipitation of wettest Month
		BIO 14	Precipitation of driest Month
		BIO 15	Precipitation seasonality (coefficient of variation)
		BIO 16	Precipitation of wettest quarter
		BIO 17	Precipitation of driest quarter
		BIO 18	Precipitation of warmest quarter
		BIO 19	Precipitation of coldest quarter
Soil data	ISRIC-WISE30sec	ALSAT	Aluminum saturation (as % of ECEC)
		BSAT	Base saturation (as % of CECsoil)
		BULK	Bulk density
		CECC	Cation exchange capacity of clay size fraction (CECclay)
		CECS	Cation exchange capacity (CECsoil)
		CFRAG	Coarse fragments (>2 mm; volume %)
		CLPC	Clay (mass %)
		CNrt	C/N ratio
		ECEC	Effective cation exchange capacity
		ELCO	Electrical conductivity
		ESP	Exchangeable sodium percentage
		GYPS	Gypsum content
		ORGC	Organic carbon
		PHAQ	Soil reaction (PHH_2O)
		SDTO	Sand (mass %)
		STPC	Silt (mass %)
		TAWC	Available water capacity (from −33 to −1500 kPa; cm m^{-1})
		TCEQ	Total carbonate equivalent
		TEB	Total exchangeable bases
		TOTN	Total nitrogen
Topographic Variable	DEM (Digital Elevation Model)	Aspect	The aspect of samples
		Slope	The slope of samples
		Elevation	The elevation of samples

Appendix B

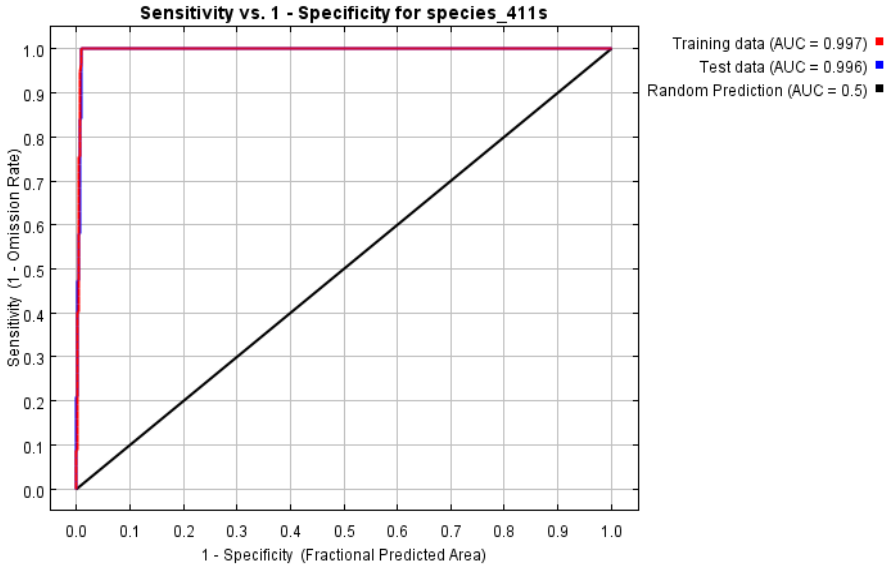

Figure A1. AUC values of MaxEnt model training data and test data.

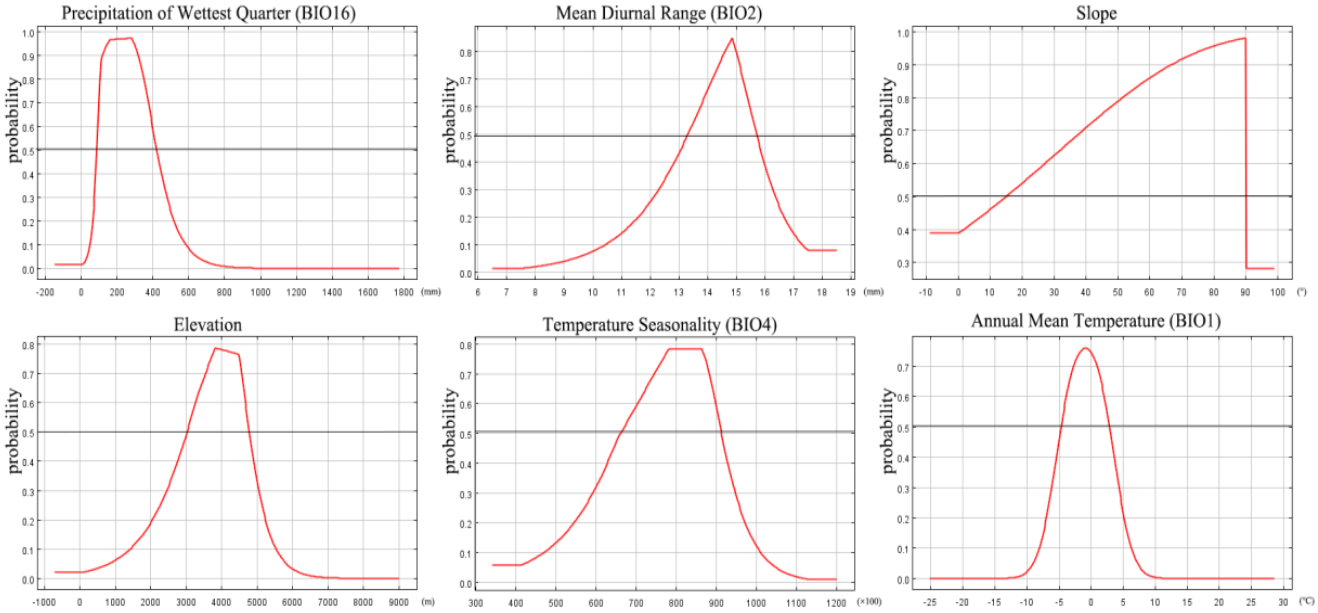

Figure A2. Response curves of major environmental factors.

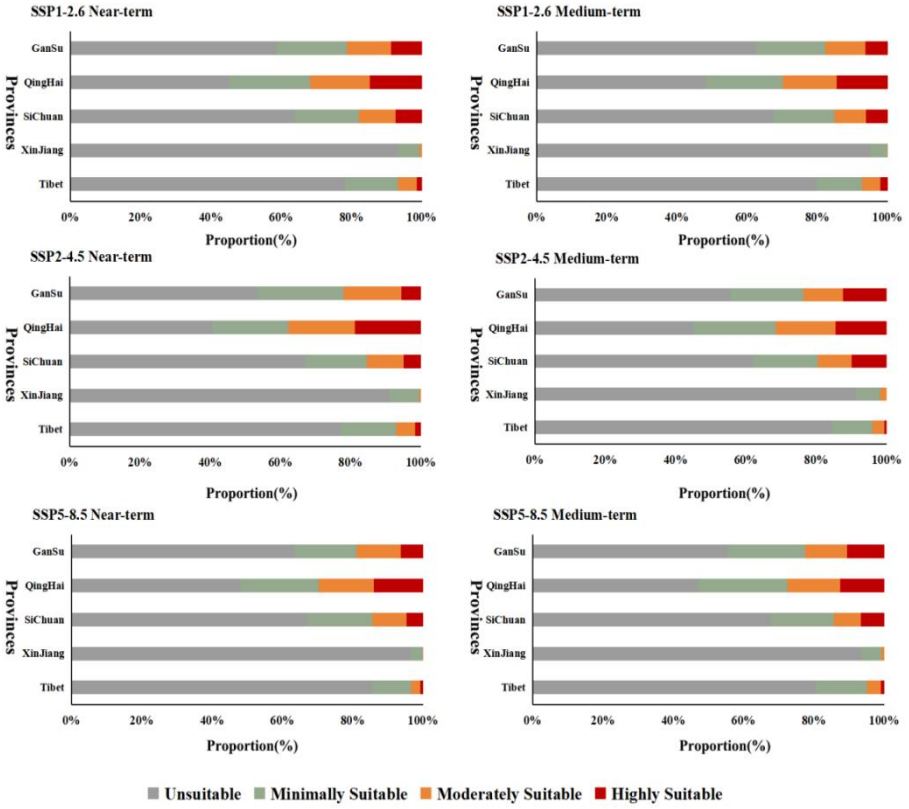

Figure A3. Proportion of suitable distribution area of *Plateau pika* in each province of Qinghai–Tibet Plateau.

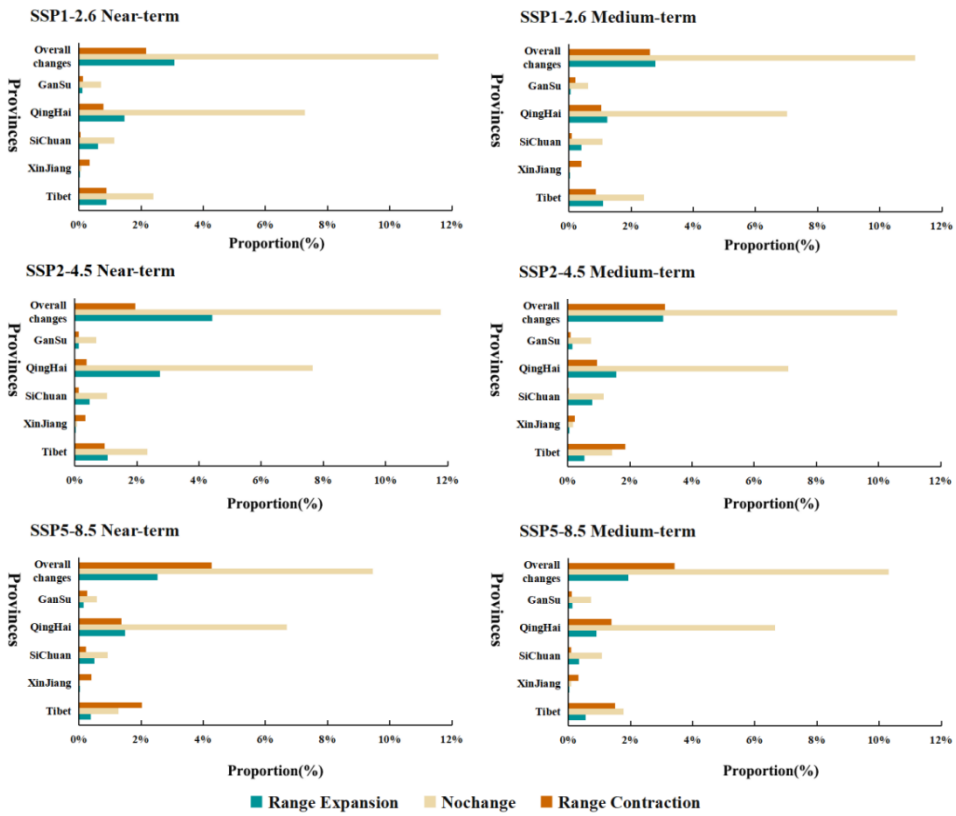

Figure A4. Expansion and contraction proportion of suitable distribution area of *Plateau pika* in each province of Qinghai–Tibet Plateau.

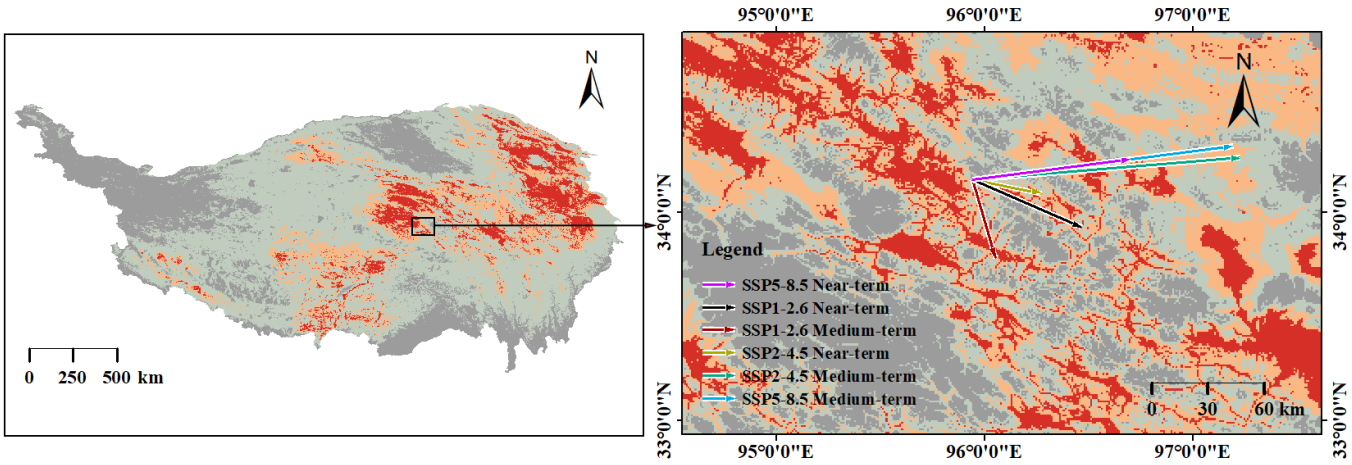

Figure A5. Characteristics of centroid migration in the suitable distribution area of *Plateau pika* under different climatic conditions in different periods.

References

1. Masson-Delmotte, V.; Zhai, P.M.; Pirani, A. *Climate Change 2021: The Physical Science Basis*; Cambridge University Press: Cambridge, UK, 2021; pp. 3–31.
2. Chen, F.H.; Wang, Y.F.; Zhen, X.L.; Sun, J. Research on the Environment Impact of the Qinghai-Tibet Plateau under Global Change and the Countermeasures. *China Tibetol.* **2021**, *4*, 21–28. (In Chinese)
3. Li, B.; He, G.; Guo, S.; Hou, R.; Huang, K.; Zhang, P.; Zhang, H.; Pan, R.; Chapman, C.A. Macaques in China: Evolutionary dispersion and subsequent development. *Am. J. Primatol.* **2020**, *82*, e23142. [CrossRef] [PubMed]
4. Chen, K.; Wang, B.; Chen, C.; Zhou, G. MaxEnt Modeling to Predict the Current and Future Distribution of *Pomatosace filicula* under Climate Change Scenarios on the Qinghai–Tibet Plateau. *Plants* **2022**, *11*, 670. [CrossRef] [PubMed]
5. Liu, L.; Zhang, Y.; Huang, Y.; Zhang, J.; Mou, Q.; Qiu, J.; Wang, R.; Li, Y.; Zhang, D. Simulation of potential suitable distribution of original species of *Fritillariae Cirrhosae Bulbus* in China under climate change scenarios. *Environ. Sci. Pollut. Res. Int.* **2022**, *29*, 22237–22250. [CrossRef]
6. Wei, Y.; Zhang, J.; Wang, J.; Wang, W. Chinese caterpillar fungus (*Ophiocordyceps sinensis*) in China: Current distribution, trading, and futures under climate change and overexploitation. *Sci. Total Environ.* **2020**, *755*, 142548. [CrossRef]
7. Huang, X.; Ma, L.; Chen, C.; Zhou, H.; Yao, B.; Ma, Z. Predicting the Suitable Geographical Distribution of *Sinadoxa Corydalifolia* under Different Climate Change Scenarios in the Three-River Region Using the MaxEnt Model. *Plants* **2020**, *9*, 1015. [CrossRef]
8. Su, J.; Aryal, A.; Nan, Z.; Ji, W. Climate Change-Induced Range Expansion of a Subterranean Rodent: Implications for Rangeland Management in Qinghai-Tibetan Plateau. *PLoS ONE* **2015**, *10*, e0138969. [CrossRef]
9. Li, R. Protecting rare and endangered species under climate change on the Qinghai Plateau, China. *Ecol. Evol.* **2019**, *9*, 427–436. [CrossRef]
10. Smith, A.T.; Badingqiuying; Wilson, M.C.; Hogan, B.W. Functional-trait ecology of the plateau pika (*Ochotona curzoniae*) in the Qinghai-Tibetan Plateau ecosystem. *Integr. Zoöl.* **2018**, *14*, 87–103. [CrossRef]
11. Smith, A.T.; Foggin, J.M. The plateau pika (*Ochotona curzoniae*) is a keystone species for biodiversity on the Tibetan plateau. *Anim. Conserv.* **1999**, *2*, 235–240. [CrossRef]
12. Zhang, W.N.; Jing, S.; Yu, C.; Pang, X.P.; Wang, J.; Guo, Z.G. Influence of the density of burrow entrances of plateau pika on the concentration of soil nutrients in a Kobresia pygmaea meadow. *Pratacult. Sci.* **2018**, *35*, 1593–1601.
13. Li, J.; Chen, Y.-Y.; Qiao, F.-Y.; Zhi, D.-G.; Guo, Z.-G. Effects of disturbance by plateau pika on the β diversity of an alpine meadow. *Chin. J. Plant Ecol.* **2021**, *45*, 476–486. [CrossRef]
14. Lai, C.H.; Smith, A.T. Keystone status of plateau pikas (*Ochotona curzoniae*): Effect of control on biodiversity of native birds. *Biodivers. Conserv.* **2003**, *12*, 1901–1912. [CrossRef]
15. Li, L.-X.; Yi, X.-F.; Li, M.-C.; Zhang, X.-A. Analysis of diets of upland buzzards using stable carbon and nitrogen isotopes. *Isr. J. Zoöl.* **2004**, *50*, 75–85. [CrossRef]
16. Hornskov, J.; Foggin, M. Brief notes on the Altai weasel Mustela altaica on the Tibetan Plateau. *Small Carniv. Conserv.* **2007**, *36*, 48–49.
17. Wu, L.; Li, J.; Lu, Z.; Schaller, G.B. Seasonal food habits and human conflict of brown bears in the Sanjiangyuan Nature Reserve, Qinghai–Tibetan Plateau, China. *Int. Bear News* **2013**, *22*, 20–21.
18. Chen, J.; Yi, S.; Qin, Y. The contribution of plateau pika disturbance and erosion on patchy alpine grassland soil on the Qinghai-Tibetan Plateau: Implications for grassland restoration. *Geoderma* **2017**, *297*, 1–9. [CrossRef]
19. Elith, J.; Leathwick, J.R. Species Distribution Models: Ecological Explanation and Prediction Across Space and Time. *Annu. Rev. Ecol. Evol. Syst.* **2009**, *40*, 677–697. [CrossRef]

20. Phillips, S.J.; Anderson, R.P.; Schapire, R.E. Maximum entropy modeling of species geographic distributions. *Ecol. Model.* **2006**, *190*, 231–259. [CrossRef]
21. Hu, F.J.; Wang, Y.; Zhang, D.; Yu, W.; Chen, G.; Xie, T.; Liu, Z.; Ma, Z.; Du, J.; Chao, B.; et al. Mapping the potential of mangrove forest restoration based on species distribution models: A case study in China. *Sci. Total Environ.* **2020**, *748*, 142321. [CrossRef]
22. Sánchez-Mercado, A.; Rodriguez-Clark, K.; Miranda, J.; Ferrer-Paris, J.R.; Coyle, B.; Toro, S.; Cardozo-Urdaneta, A.; Braun, M.J. How to deal with ground truthing affected by human-induced habitat change?: Identifying high-quality habitats for the Critically Endangered Red Siskin. *Ecol. Evol.* **2018**, *8*, 841–851. [CrossRef] [PubMed]
23. Ma, W.; Ding, J.; Wang, R.; Wang, J. Drivers of PM2.5 in the urban agglomeration on the northern slope of the Tianshan Mountains, China. *Environ. Pollut.* **2022**, *309*, 119777. [CrossRef] [PubMed]
24. Sand-Jensen, K.; Borum, J.; Møller, C.L.; Baastrup-Spohr, L. Physiological Adaptation and Plant Distribution along a Steep Hydrological Gradient. *Plants* **2022**, *11*, 1683. [CrossRef] [PubMed]
25. Early, R.; Rwomushana, I.; Chipabika, G.; Day, R. Comparing, evaluating and combining statistical species distribution models and CLIMEX to forecast the distributions of emerging crop pests. *Pest Manag. Sci.* **2021**, *78*, 671–683. [CrossRef] [PubMed]
26. Elith, J.H.; Graham, C.P.H.; Anderson, R.P.; Dudík, M.; Ferrier, S.; Guisan, A.; Hijmans, R.J.; Huettmann, F.; Leathwick, J.R.; Lehmann, A.; et al. Novel methods improve prediction of species' distributions from occurrence data. *Ecography* **2006**, *29*, 129–151. [CrossRef]
27. Zhang, D.; An, B.; Chen, L.; Sun, Z.; Mao, R.; Zhao, C.; Zhang, L. Camera Trapping Reveals Spatiotemporal Partitioning Pat-terns and Conservation Implications for Two Sympatric Pheasant Species in the Qilian Mountains, Northwestern China. *Animals* **2022**, *28*, 12.
28. Lu, K.; He, Y.-M.; Mao, W.; Du, Z.-Y.; Wang, L.-J.; Liu, G.-M.; Feng, W.-J.; Duan, Y.-Z. Potential geographical distribution and changes of *Artemisia ordosica* in China under future climate change. *J. Appl. Ecol.* **2020**, *31*, 3758–3766.
29. Zahoor, B.; Liu, X.; Ahmad, B.; Kumar, L.; Songer, M. Impact of climate change on Asiatic black bear (*Ursus thibetanus*) and its autumn diet in the northern highlands of Pakistan. *Glob. Chang. Biol.* **2021**, *27*, 4294–4306. [CrossRef]
30. Xia, X.; Li, Y.; Yang, D.; Pi, Y. Rana hanluica. Potential geographical distribution of in China under climate change. *Ying Yong Sheng Tai Xue Bao* **2021**, *32*, 4307–4314. [CrossRef]
31. Evcin, O.; Kucuk, O.; Akturk, E. Habitat suitability model with maximum entropy approach for European roe deer (*Capreolus capreolus*) in the Black Sea Region. *Environ. Monit. Assess.* **2019**, *191*, 669. [CrossRef]
32. Zhang, Y.L.; Li, B.Y.; Zheng, D. A discussion on the boundary and area of the Tibetan Plateau in China. *Geogr. Res.* **2002**, *21*, 1–9. (In Chinese)
33. Qiu, J. The third pole. *Nature* **2008**, *454*, 393–396. [CrossRef] [PubMed]
34. Myers, N.; Mittermeier, R.A.; Mittermeier, C.G.; da Fonseca, G.A.B.; Kent, J. Biodiversity hotspots for conservation priorities. *Nature* **2000**, *403*, 853–858. [CrossRef]
35. Wilson, E.O. *The Diversity of Life*; Harvard University Press: Cambridge, MA, USA, 1992; pp. 125–135.
36. Fu, B.J.; Ouyang, Z.Y.; Shi, P.; Fan, J.; Wang, X.D.; Zheng, H.; Zhao, W.; Wu, F. Current Condition and Protection Strategies of Qinghai-Tibet Plateau. *Ecol. Secur. Barrier Policy Manag. Res.* **2021**, *36*, 1298–1306. (In Chinese) [CrossRef]
37. Lobo, J.M.; Jiménez-Valverde, A.; Real, R. AUC: A misleading measure of the performance of predictive distribution models. *Glob. Ecol. Biogeogr.* **2008**, *17*, 145–151. [CrossRef]
38. He, Y.; Lin, G.; Ci, H.; Liu, C.; Zhang, T.; Su, J. The past population dynamics of Ochotona curzoniae and the response to the climate change. *North-West. J. Zool.* **2018**, *14*, 220–225.
39. Evans, A.; Jacquemyn, H. Impact of mating system on range size and niche breadth in Epipactis (*Orchidaceae*). *Ann. Bot.* **2020**, *126*, 1203–1214. [CrossRef]
40. Boria, R.A.; Olson, L.E.; Goodman, S.M.; Anderson, R.P. Spatial filtering to reduce sampling bias can improve the performance of ecological niche models. *Ecol. Model.* **2014**, *275*, 73–77. [CrossRef]
41. Calkins, M.T.; Beever, E.A.; Boykin, K. Not-so-splendid isolation: Modeling climate-mediated range collapse of a montane mammal (*Ochotona princeps*) across the Western United States. *Ecography* **2012**, *35*, 780–791. [CrossRef]
42. Wang, M.; Zhang, C.; Mi, C.; Han, L.; Li, M.; Xu, W.; Yang, W. Potential impacts of climate change on suitable habitats of Marco Polo sheep in China. *Ying Yong Sheng Tai Xue Bao* **2021**, *32*, 3127–3135. [CrossRef]
43. Dai, Y. The overlap of suitable tea plant habitat with Asian elephant (*Elephus maximus*) distribution in southwestern China and its potential impact on species conservation and local economy. *Environ. Sci. Pollut. Res.* **2021**, *29*, 5960–5970. [CrossRef]
44. Dong, X.; Chu, Y.-M.; Gu, X.; Huang, Q.; Zhang, J.; Bai, W. Suitable habitat prediction of Sichuan snub-nosed monkeys (*Rhinopithecus roxellana*) and its implications for conservation in Baihe Nature Reserve, Sichuan, China. *Environ. Sci. Pollut. Res.* **2019**, *26*, 32374–32384. [CrossRef] [PubMed]
45. Galiano, D.; Bernardo-Silva, J.; De Freitas, T.R.O. Genetic Pool Information Reflects Highly Suitable Areas: The Case of Two Parapatric Endangered Species of Tuco-tucos (*Rodentia: Ctenomiydae*). *PLoS ONE* **2014**, *9*, e97301. [CrossRef]
46. Boer, G.J.; Smith, D.M.; Cassou, C.; Doblas-Reyes, F.; Danabasoglu, G.; Kirtman, B.; Kushnir, Y.; Kimoto, M.; Meehl, G.A.; Msadek, R.; et al. The Decadal Climate Prediction Project (DCPP) contribution to CMIP6. *Geosci. Model Dev.* **2016**, *9*, 3751–3777. [CrossRef]
47. Zhou, T.J.; Zou, L.W.; Chen, X.L. Commentary on the Coupled Model Intercomparison Project Phase 6 (CMIP 6). *Clim. Change Res.* **2019**, *15*, 445–456. [CrossRef]

48. IPCC. *Climate Change 2013: The Physical Science Basis: Contribution of Working Group I to the Fifth Assessment Report of the Intergovernmental Panel on Climate Change*; Cambridge University Press: Cambridge, MA, USA, 2013; pp. 1–1535.
49. Wang, L.; Bao, Q.; He, H. Short commentary on CMIP6 High Resolution Model Intercomparison Project (HighResMIP). *Adv. Clim. Change Res.* **2019**, *15*, 498–502.
50. Wu, B.; Xin, X.G. Short commentary on CMIP6 Decadal Climate Prediction Project (DCPP). *Adv. Clim. Change Res.* **2019**, *15*, 476–480.
51. Su, B.; Huang, J.; Mondal, S.K.; Zhai, J.; Wang, Y.; Wen, S.; Gao, M.; Lv, Y.; Jiang, S.; Jiang, T.; et al. Insight from CMIP6 SSP-RCP scenarios for future drought characteristics in China. *Atmos. Res.* **2020**, *250*, 105375. [CrossRef]
52. Batjes, N.H. World Soil Property Estimates for Broad-Scale Modelling (WISE30sec). Report 2015/01, ISRIC—World Soil Information, Wageningen. 2015. Available online: https://www.isric.org/sites/default/files/isric_report_2015_01.pdf (accessed on 6 April 2022).
53. Wei, W.; Zhang, L.; Yang, G.; Xu, J.; Fan, X.; Zhang, W. Characteristics and functions of pika burrows in plateau. *Acta Pratacult. Sin.* **2013**, *22*, 198–204.
54. Ying, X.; Hai, X.C. Preliminary assessment of simulations of climate changes over China by CMIP5 multimodels. *Atmos. Ocean. Sci. Lett.* **2012**, *5*, 489–494. [CrossRef]
55. Eyring, V.; Cox, P.M.; Flato, G.M.; Gleckler, P.J.; Abramowitz, G.; Caldwell, P.; Collins, W.D.; Gier, B.K.; Hall, A.D.; Hoffman, F.M.; et al. Taking climate model evaluation to the next level. *Nat. Clim. Chang.* **2019**, *9*, 102–110. [CrossRef]
56. Kim, H.-Y.; Ko, J.; Kang, S.; Tenhunen, J. Impacts of climate change on paddy rice yield in a temperate climate. *Glob. Chang. Biol.* **2013**, *19*, 548–562. [CrossRef]
57. Su, P.; Zhang, A.; Wang, R.; Wang, J.; Gao, R.; Liu, F. Prediction of Future Natural Suitable Areas for Rice under Representative Concentration Pathways (RCPs). *Sustainability* **2021**, *13*, 1580. [CrossRef]
58. Ma, W.; Jia, W.; Zhou, Y.; Liu, F.; Wang, J. Prediction of Suitable Future Natural Areas for Highland Barley on the Qinghai-Tibet Plateau under Representative Concentration Pathways (RCPs). *Sustainability* **2022**, *14*, 6617. [CrossRef]
59. Peterson, A.T.; Papeş, M.; Soberón, J. Rethinking receiver operating characteristic analysis applications in ecological niche modeling. *Ecol. Model.* **2008**, *213*, 63–72. [CrossRef]
60. Warren, D.L.; Seifert, S.N. Ecological niche modeling in Maxent: The importance of model complexity and the performance of model selection criteria. *Ecol. Appl.* **2011**, *21*, 335–342. [CrossRef]
61. Zhu, G.; Qiao, H. Effect of the Maxent model's complexity on the prediction of species potential distributions. *Biodivers. Sci.* **2016**, *24*, 1189–1196. [CrossRef]
62. Cobos, M.E.; Townsend Peterson, A.; Barve, N.; Osorio-Olvera, L. kuenm: An R package for detailed development of ecological niche models using Maxent. *PeerJ* **2019**, *7*, e6281. [CrossRef] [PubMed]
63. Phillips, S.J.; Dudík, M. Modeling of species distributions with Maxent: New extensions and a comprehensive evaluation. *Ecography* **2008**, *31*, 161–175. [CrossRef]
64. Tarabon, S.; Bergès, L.; Dutoit, T.; Isselin-Nondedeu, F. Environmental impact assessment of development projects im-proved by merging species distribution and habitat connectivity modelling. *J. Environ. Manag.* **2019**, *241*, 439–449. [CrossRef]
65. Anderson, R.P.; Lew, D.; Peterson, A. Evaluating predictive models of species' distributions: Criteria for selecting optimal models. *Ecol. Model.* **2003**, *162*, 211–232. [CrossRef]
66. Thapa, A.; Wu, R.; Hu, Y.; Nie, Y.; Singh, P.B.; Khatiwada, J.R.; Yan, L.; Gu, X.; Wei, F. Predicting the potential distribution of the endangered red panda across its entire range using MaxEnt modeling. *Ecol. Evol.* **2018**, *8*, 10542–10554. [CrossRef]
67. Wang, Y.; Zhang, X.; Sun, Y.; Chang, S.; Wang, Z.; Li, G.; Hou, F. Pika burrow and zokor mound density and their relationship with grazing management and sheep production in alpine meadow. *Ecosphere* **2020**, *11*, e03088. [CrossRef]
68. Zhang, L.; Wei, Y.Q.; Wang, J.N.; Zhou, Q.; Liu, F.G.; Chen, Q.; Liu, F. The potential geographical distribution of Lycium ru-thenicum Murr under different climate change scenarios. *Chin. J. Appl. Envion. Biol.* **2020**, *26*, 969–978.
69. Wu, Y.-N.; Ma, Y.-J.; Liu, W.-L.; Zhang, W.-Z. Modeling the Spatial Distribution of Plateau Pika (*Ochotona curzoniae*) in the Qinghai Lake Basin, China. *Animals* **2019**, *9*, 843. [CrossRef]
70. Muscarella, R.; Galante, P.J.; Soley-Guardia, M.; Boria, R.A.; Kass, J.M.; Uriarte, M.; Anderson, R.P. ENMeval: An R package for conducting spatially independent evaluations and estimating optimal model complexity for MaxEnt ecological niche models. *Methods Ecol. Evol.* **2014**, *5*, 1198–1205. [CrossRef]
71. Smith, A.T. The Distribution and Dispersal of Pikas: Influences of Behavior and Climate. *Ecology* **1974**, *55*, 1368–1376. [CrossRef]
72. Solari, K.A.; Hadly, E.A. Evolution for extreme living: Variation in mitochondrial cytochrome c oxidase genes correlated with elevation in pikas (*genus Ochotona*). *Integr. Zool.* **2018**, *13*, 517–535. [CrossRef]
73. Richalet, J.P.; Voituron, N.; Hermand, E. Chemoreflexes: A Major Component of Adaptation to High Altitude/Hypoxic Environment. *FASEB J.* **2017**, *31*, 841–849.
74. Li, Y.; Wang, Z.; Zhang, X.; Shi, L. Analysis of dominant factors affecting microhabitat selection of plateau pika (*Ochotona curzoniae)* during summer in Altun Mountain National Nature Reserve, Xinjiang Uygur Autonomous Region, China. *Chin. J. Vector Biol. Control. Febr.* **2014**, *25*, 1. [CrossRef]
75. Andersen, D.C. Geomys Bursarius Burrowing Patterns: Influence of Season and Food Patch Structure. *Ecology* **1987**, *68*, 1306–1318. [CrossRef]

76. Fissore, C.; Giardina, C.P.; Kolka, R.K.; Trettin, C.C.; King, G.M.; Jurgensen, M.F.; Barton, C.D.; McDowell, S.D. Temperature and vegetation effects on soil organic carbon quality along a forested mean annual temperature gradient in North America. *Glob. Chang. Biol.* **2007**, *14*, 193–205. [CrossRef]
77. Wei, W.R. The Study of Habitat Burrow Features and Functions of the Plateau Pika. Ph.D. Thesis, Lanzhou University, Lanzhou, China, 2013. (In Chinese).
78. Tang, Z.H.; Luo, H.L.; Wang, J.H.; Liu, J.L.; You, Z.Q. Potential suitable habitat and protection gap analysis of White-lipped deer (*Cervus albirosrostris*) based on GIS and MaxEnt model. *Acta Ecol. Sin.* **2022**, *22*, 1–10.
79. Wu, X.; Dong, S.; Liu, S. Predicting the shift of threatened ungulates' habitats with climate change in Altun Mountain National Nature Reserve of the Northwestern Qinghai-Tibetan Plateau. *Clim. Chang.* **2017**, *142*, 331–344. [CrossRef]
80. Song, C.-Q.; You, S.-C.; Ke, L.-H.; Liu, G.-H.; Zhong, X.-K. Spatio-temporal variation of vegetation phenology in the Northern Tibetan Plateau as de-tected by MODIS remote sensing. *Chin. J. Plant Ecol.* **2011**, *35*, 853–863. [CrossRef]
81. Liu, Z.; Li, S.; Wei, W.; Song, X. Research progress on alpine wetland changes and driving forces in Qinghai-Tibet Plateau during the last three decades. *Chin. J. Ecol.* **2019**, *38*, 856–862. (In Chinese) [CrossRef]
82. Luo, Z.; Jiang, Z.G.; Tang, S. Impacts of climate change on distributions and diversity of ungulates on the Tibetan Plateau. *Ecol. Appl.* **2015**, *25*, 24–38. (In Chinese) [CrossRef] [PubMed]
83. Zhao, W.; Chen, H.; Liu, L.; Qi, M.; Zhang, J.; Du, T.; Jin, L. The Impact of Climate Change on the Distribution Pattern of the Suitable Growing Region for Endangered Tibetan Medicine Meconopsis punicea. *Chin. Pharm. J.* **2021**, *56*, 16. (In Chinese)